

Saw-tooth softening/stiffening - a stable computational procedure for RC structures

Jan G. Rots[†]

*Faculty of Architecture and Faculty of Civil Engineering & Geosciences, Delft University of Technology,
P.O.Box 5043, 2600 GA - Delft, The Netherlands*

Stefano Invernizzi[‡]

*Department of Structural Engineering and Geotechnics, Politecnico di Torino,
Corso Duca degli Abruzzi 24, 10129 - Torino, Italy. Also research fellow at TUDelft.*

Beatrice Belletti^{‡†}

*Department of Civil and Environmental Engineering and Architecture, University of Parma,
Parco Area delle Scienze 181/a, 43100 - Parma, Italy. Also research fellow at TUDelft.*

(Received December 21, 2005, Accepted May 3, 2006)

Abstract. Over the past years techniques for non-linear analysis have been enhanced significantly via improved solution procedures, extended finite element techniques and increased robustness of constitutive models. Nevertheless, problems remain, especially for real world structures of softening materials like concrete. The softening gives negative stiffness and risk of bifurcations due to multiple cracks that compete to survive. Incremental-iterative techniques have difficulties in selecting and handling the local peaks and snap-backs. In this contribution, an alternative method is proposed. The softening diagram of negative slope is replaced by a saw-tooth diagram of positive slopes. The incremental-iterative Newton method is replaced by a series of linear analyses using a special scaling technique with subsequent stiffness/strength reduction per critical element. It is shown that this event-by-event strategy is robust and reliable. First, the model is shown to be objective with respect to mesh refinement. Next, the example of a large-scale dog-bone specimen in direct tension is analyzed using an isotropic version of the saw-tooth model. The model is capable of automatically providing the snap-back response. Subsequently, the saw-tooth model is extended to include anisotropy for fixed crack directions to accommodate both tensile cracking and compression strut action for reinforced concrete. Three different reinforced concrete structures are analyzed, a tension-pull specimen, a slender beam and a slab. In all cases, the model naturally provides the local peaks and snap-backs associated with the subsequent development of primary cracks starting from the rebar. The secant saw-tooth stiffness is always positive and the analysis always 'converges'. Bifurcations are prevented due to the scaling technique.

Keywords: softening; saw-tooth softening; snap-back; sequentially linear analysis; cracking; fracture; reinforced concrete.

[†] Full Professor, Corresponding Author, E-mail: j.g.rots@bk.tudelft.nl

[‡] Assistant Professor, E-mail: stefano.invernizzi@polito.it

^{‡†} Assistant Professor, E-mail: beatrice.belletti@unipr.it

1. Introduction

Negative stiffness due to softening is a major problem in computational modelling of concrete structures. It may lead to numerical instability and divergence of the incremental-iterative procedure. This holds especially for the analysis of medium- and large-scale *structures*. Cracks in structures are accompanied by dips, ripples, jumps and snap-backs in the load-displacement response. This behaviour is typical of *un-reinforced* structures (e.g. facades) where the amount of elastic energy stored in the structure is large compared to the fracture energy consumed in crack or crush propagation, but also of *reinforced* structures (e.g. RC beams, plates and shells) where each primary crack gives a release or drop followed by a new ascending portion in the load-displacement curve. Multiple cracks occur that compete to survive. To try and solve such problems, users have to resort to arc-length or indirect control schemes (e.g. De Borst 1987) which is cumbersome and often inadequate when the bifurcations are multiple, the peaks irregular or the snap-backs sharp (Crisfield 1982). When using discrete cohesive cracks, convergence can sometimes be achieved by using CMOD control or by using the crack length as the control parameter (e.g. Carpinteri 1986, Carpinteri and Monetto 1999). Otherwise, the above mentioned problems arise, independently of the type of smeared crack formulation adopted, either decomposed-strain, total-strain, damage or plasticity based crack models.

As an alternative, this paper presents a sequentially linear saw-tooth continuum model which captures the nonlinear response via a series of linear steps. The softening stress-strain curve with negative slope is replaced by a saw-tooth diagram of positive slopes, while the incremental-iterative procedure is replaced by a scaled sequentially linear procedure (Rots 2001). After a linear analysis, the critical element, i.e., the element for which the stress is most close to the current peak in the saw-tooth diagram, is traced. Next, the strength and stiffness of that element are reduced and the process is repeated. The sequence of critical states governs the global load-displacement response, while the elements with reduced stiffness reveal the softened areas. The advantage is that there is no such thing as ‘negative incremental stiffness’, as the secant linear (saw-tooth) stiffness is always positive. The analysis always ‘converges’. Mesh-size objectivity is achieved by adjusting both the peaks and the ultimate strain of the saw-tooth diagram to the size of the finite elements, keeping the fracture energy invariant (Rots and Invernizzi 2004).

The paper starts with a summary of the description of the model. Subsequently, the case of large-scale dog-bone specimens in direct tension is considered. It will be demonstrated that the sequentially linear model is capable of automatically providing the snap-back response. Bifurcations in these symmetric fracture specimens are circumvented in a natural manner as the scaling procedure always picks the ‘lowest’ equilibrium solution associated with the ‘most critical’ element, even for numerical round-off in a symmetric case.

Finally, the model is improved to take into account the intrinsic anisotropy due to crack nucleation and softening. This is a crucial aspect in order to describe reinforced structures, in which the reinforcement *ties* are balanced against concrete compressive *struts* that develop parallel to the crack directions.

Three different reinforced structures are considered, namely a reinforced tension-pull specimen, a slender reinforced concrete beam and a reinforced concrete slab. In all cases, the response shows local peaks and snap-backs associated with the subsequent development of primary cracks starting from the rebar. Comparisons between incremental-iterative solutions and sequentially linear solutions are given and the behaviour is interpreted in terms of load-displacement response and crack patterns.

2. Isotropic saw-tooth softening

2.1. Global sequentially linear procedure

The basic idea is to look for the equilibrium configuration via secant approximations with restarts from the origin. The softening diagram is approximated by a saw-tooth curve and linear analyses are carried out sequentially (Rots 2001). The global procedure is as follows. The structure is discretized using standard elastic continuum elements with assigned tensile strength. Subsequently, the following steps are carried out:

- Add the external load as a unit load.
 - Perform a linear elastic analysis.
 - Extract the critical element from the results. The critical element is the element for which the principal tensile stress is closest to its current strength. This principal tensile stress criterion is widely accepted in mode-I fracture mechanics of quasi-brittle materials.
 - Calculate the critical global load as the unit load times the current strength divided by stress of the critical element.
 - Extract also a corresponding global displacement measure, so that later an overall load-displacement curve can be constructed.
 - Reduce the stiffness and strength, i.e., Young's modulus E and tensile strength f_t of the critical element, according to a saw-tooth tensile softening stress strain curve as described in the following.
 - Repeat the previous steps for the new configuration, i.e. re-run a linear analysis for the structure in which E and f_t of the previous critical element are reduced.
- Repeat again, etc.

There is some similarity with fracture analysis on lattices (e.g. Schlangen and van Mier 1992, Beranek and Hobbelman 1995), where little beam elements are removed rather than continuum elements reduced. The advantage of using continua with saw-tooth softening rather than brittle lattice elements is that engineering notions like principal stress, strength and fracture energy are preserved and that the macro-toughness at structural level can be simulated in a natural way.

2.2. Saw-tooth softening model via stepwise reduction of Young's modulus

The way in which the stiffness and strength of the critical elements are progressively reduced constitutes the essence of the model. A very rough method would be to reduce E to zero immediately after the first, initial strength is reached. This elastic perfectly brittle approach, however, is likely to be mesh dependent as it will not yield the correct energy consumption upon mesh refinement (Bažant and Cedolin 1979). In this study, the consecutive strength and stiffness reduction is based upon the concept of tensile strain softening, which is fairly accepted in the field of fracture mechanics of concrete (Bažant and Oh 1983).

The tensile softening stress-strain curve is defined by Young's modulus E , the tensile strength f_t , the shape of the diagram, e.g., a linear or exponential diagram, and the area under the diagram. The area under the diagram represents the fracture energy G_f divided by the crack band width h , which is a discretisation parameter associated with the size, orientation and integration scheme of the finite element. Although there is some size-dependence, the fracture energy can be considered to be a

material property. This softening model usually governs nonlinear constitutive behavior in an incremental-iterative strategy. Please note that here we adopt the curve only as a ‘mother’ or envelope curve that determines the consecutive strength reduction in sequentially linear analysis. In the present study, attention is confined to a linear softening diagram, but extension to any other shape of the diagram is possible. For a linear softening diagram, the ultimate strain ε_u of the diagram reads:

$$\varepsilon_u = \frac{2G_f}{f_t h} \quad (1)$$

In a sequentially linear strategy, the softening diagram can be imitated by consecutively reducing Young’s modulus as well as the strength. Young’s modulus can e.g., be reduced according to:

$$E_i = \frac{E_{i-1}}{a}, \text{ for } i = 1 \text{ to } N \quad (2)$$

with i denoting the current stage in the saw-tooth diagram, $i-1$ denoting the previous stage in the saw-tooth diagram and a being a constant. When a is taken as 2, Young’s modulus of a critical element is reduced by a factor 2 compared to the previous state. N denotes the amount of reductions that is applied in total for an element. When an element has been critical N times, it is removed completely in the next step.

The reduced strength f_{ii} corresponding to the reduced Young’s modulus E_i is taken in accordance with the envelope softening stress-strain curve:

$$f_{ii} = \varepsilon_u E_i \frac{D}{E_i + D} \quad (3)$$

with

$$E_i = \frac{E}{a^i} \quad (4)$$

and

$$D = \frac{f_t}{\varepsilon_u - \frac{f_t}{E}} \quad (5)$$

being the tangent to the tensile stress-strain softening curve. Note that this is the softening curve in terms of stress versus *total* strain, i.e., the sum of elastic strain and crack strain of an imagined cracked continuum.

The model always provides a solution: the secant saw-tooth stiffness is always positive, so that ill-conditioning or divergence does not appear in sequentially linear analysis. An advantage of the model is that the regular notions of fracture mechanics, like the principal tensile stress criterion, the envelope strength and fracture energy are maintained which helps in reaching realistic energy consumption and toughness as observed in experiments.

2.3. Mesh regularization

The concept of smeared cracking basically assumes that the localized crack is distributed over a continuum finite element, provided that the crack opening δ is equal to the element strain ε times the

so called crack band width h (for lower-order elements often equal to the element size). In order to achieve mesh-size objectivity, the ultimate strain ε_u in smeared crack models is usually adjusted to h according to Eq. (1) for linear softening (Bažant and Oh 1993). In previous works (Rots and Invernizzi 2003), it appeared that such adjustment is not sufficient to guarantee mesh-size objectivity for the case of the sequentially linear model. In fact, due to the saw-tooth approximation of the softening curve, the dissipated energy is always less than the theoretical one, i.e., the one referring to the smooth ‘mother’ softening curve. Moreover, the underestimation of the dissipated energy depends not only on the number of teeth, but also on the mesh size, since the ultimate strain depends on the crack band width. When finer meshes are considered, i.e., for a small value of h , the slope of the linear softening branch decreases and the area underestimation becomes more important.

In order to provide a correct regularization procedure and achieve mesh independence, it is first of all necessary to provide a useful expression for the actual area beneath the saw-tooth curve. Referring to the scheme in Fig. 1, the formula is the following:

$$A = \sum_{i=0}^{N-1} A_i = \sum_{i=0}^{N-1} \frac{1}{2} \varepsilon_i f_{ii} b_i \tag{6}$$

where the index i refers to the triangular decomposition of the whole area.

The parameter b_i varies depending on the saw-tooth approximation method. In the case of stepwise Young’s modulus reduction, it is the following:

$$b_i = \begin{cases} \left(1 - \frac{1}{a}\right) & 0 \leq i < N-1 \\ 1 & i = N-1 \end{cases} \tag{7}$$

The basic idea, thus, is to update the tensile strength, or the ultimate strain, or even both, in order to keep the dissipated energy invariant. In other words, the area A^* , under the updated constitutive law, becomes invariant and equal to:

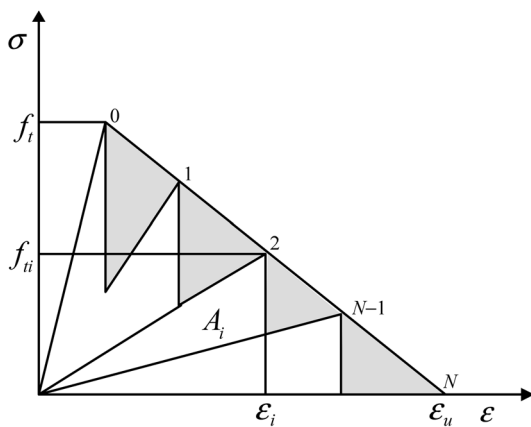


Fig. 1 Saw-tooth softening approximation scheme, the underestimated area is shown in grey

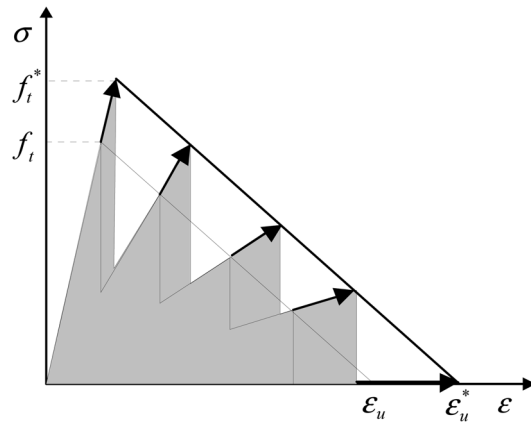


Fig. 2 Regularization scheme with both the ultimate strain and the tensile strength update, keeping constant the softening modulus D

$$A^* = \frac{G_f}{h} \quad (8)$$

Eq. (8) shows clearly that not only the number of teeth, but also the mesh size (i.e. the crack band width h) comes into play. Although in principle different approaches can be followed, it has been proved that the most effective technique is to update both the tensile strength and the ultimate strain. Therefore, the updated strength f_t^* and the ultimate strain ε_t^* will be determined as follow:

$$\begin{cases} f_t^* = k \cdot f_t \\ \varepsilon_t^* = k \cdot \varepsilon_t \end{cases} \quad (9)$$

where k can be determined numerically in such a way that the new area satisfies Eq. (8) (see Fig. 2). After some analytical manipulation of Eq. (8), a closed form expression for the parameter k can be obtained:

$$k = \frac{\sqrt{\frac{G_f}{h}}}{\sqrt{\sum_{i=0}^{N-1} \frac{1}{2} \frac{f_{ti}^2}{E_i} b_i}} \quad (10)$$

In order to show the effectiveness of the provided regularization, a symmetric notched beam of total length 500 mm, span 450 mm, height 100 mm, thickness 50 mm and notch depth 10 mm was selected for analysis. The distance between the loading points in the symmetric four-point loading scheme is 150 mm. Five different meshes were used (Fig. 3). These meshes have a symmetric

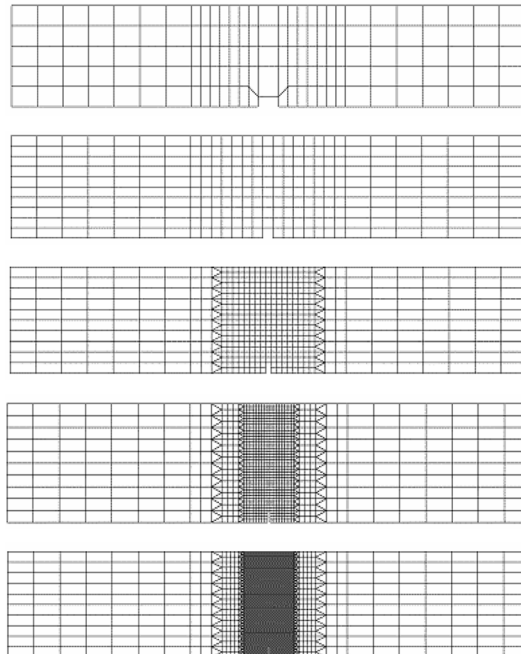


Fig. 3 Meshes considered in the analysis, respectively referred in the following as very coarse, coarse, medium, fine and very fine

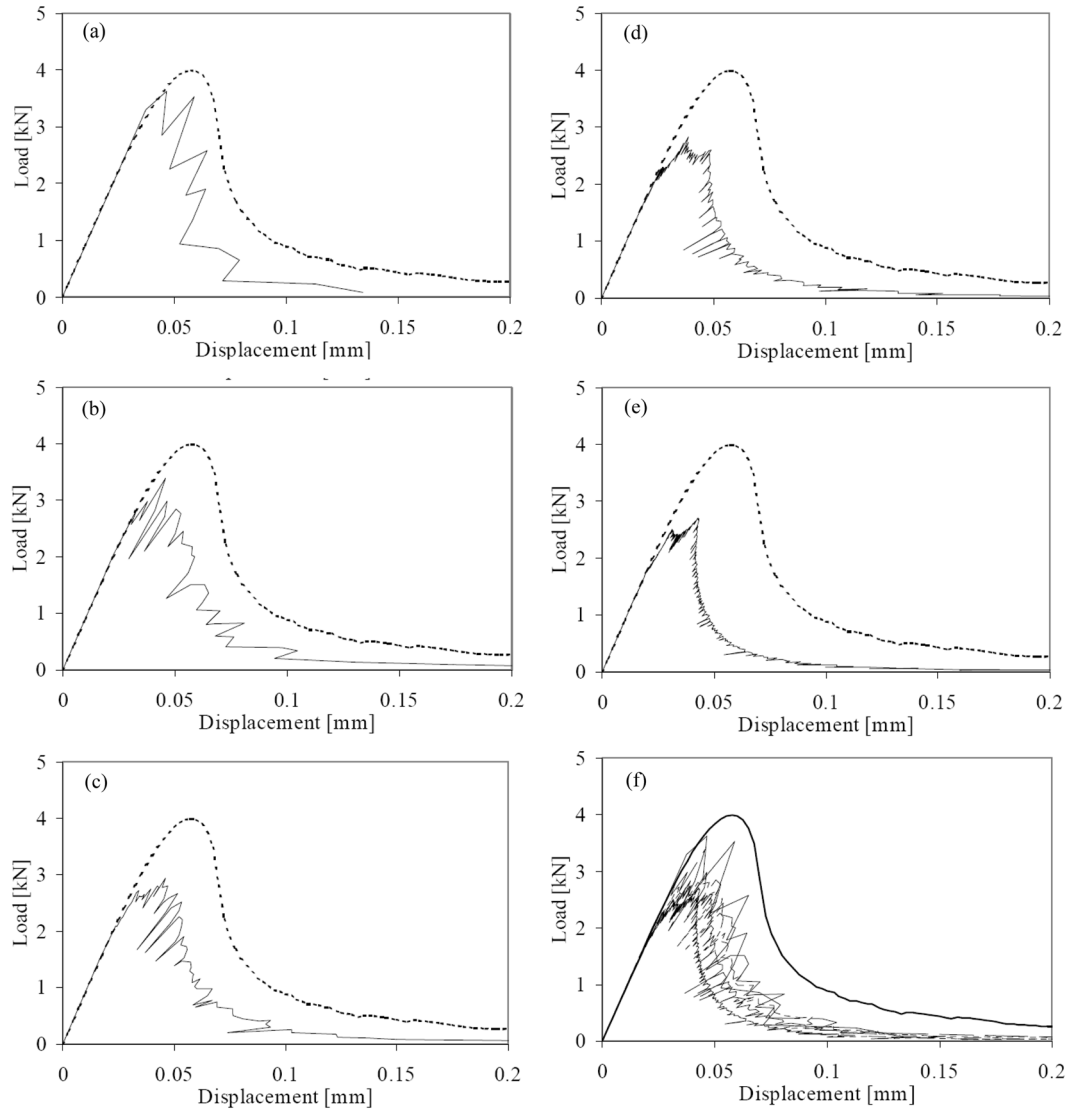


Fig. 4 Load-displacement diagrams for the un-regularized model, ten teeth, five different meshes (arranged from coarse to fine). Final plot combines all individual diagrams. The curves show quite a scatter and deviate from the non-linear reference curve (continuous line)

center crack band of 20 mm, 10 mm, 5 mm, 2.5 mm and 1.25 mm width respectively. Four-node linear elements were used.

Fig. 4 shows the load-displacement curves for the un-regularized model, for the five different meshes and a ten-teeth approximation. The curves are constructed by connecting the critical loads and the corresponding displacements for all linear analyses that have been executed sequentially. Due to the scaling process, the curves have a somewhat spiky irregular shape, but can be conceived to follow some average path. In Fig. 4 the results for the various meshes are clearly in-objective. The finer the mesh, the lower the peak load. Furthermore, the curves in Fig. 4 do not resemble the

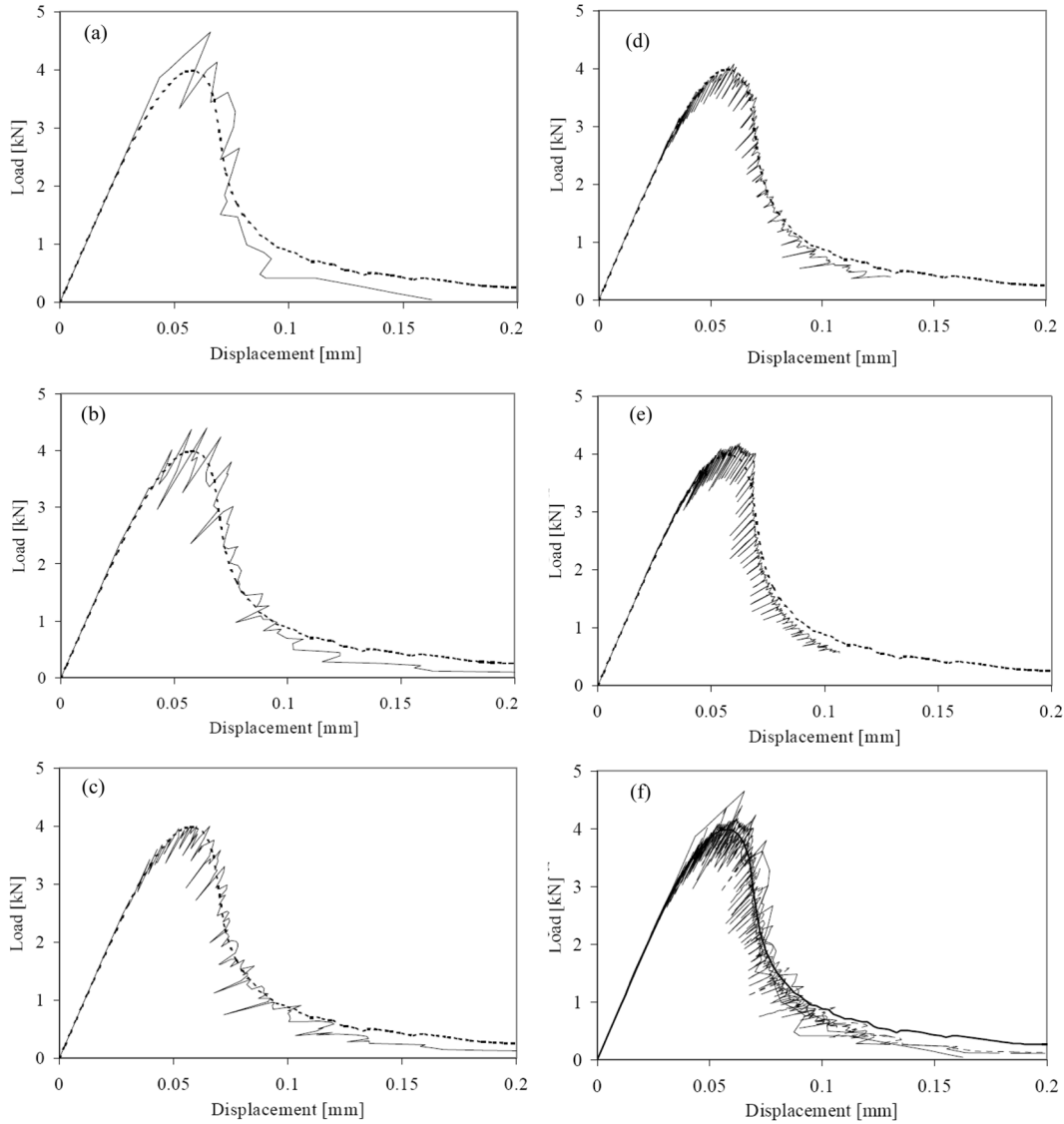


Fig. 5 Load displacement diagrams for the regularized model, ten teeth, five different meshes (arranged from coarse to fine). Final plot combines all individual diagrams. All the curves are coherent and closely resemble the reference curve and reference peak load (continuous line)

reference behavior from a nonlinear softening analysis using the same parameters. Fig. 5 shows the load-displacement curves for the regularized model, again for the five meshes and the ten-teeth approximation. In the regularized case, it is evident that the sequentially linear results are in good agreement with the nonlinear analysis regardless the mesh size. The results are now mesh-objective. A detailed demonstration of this mesh-objectivity is given in Rots and Invernizzi (2003), also for different numbers of teeth adopted. There, also a more detailed explanation of the irregular spiky nature of the curves is given.

3. Large-scale dog-bone specimens in direct tension

The case study concerns direct tensile tests carried out on large-scale dog-bone concrete specimens (Van Vliet 2000). In order to prove the ability of the saw tooth model to capture the structural snap-back, we considered the largest size among the entire series, denominated as *type F* ($D = 1600$ mm; $r = 1160$ mm). Experimental load-displacement curves, shown in Fig. 6, were obtained under indirect displacement control, adopting a gauge length that was sufficiently short. The mechanical parameters obtained by the test were adopted for the numerical analysis, i.e., a nominal tensile strength $f_t = 2.31$ Mpa and a fracture energy $G_f = 0.1411$ N/mm. A linear softening tail was assumed.

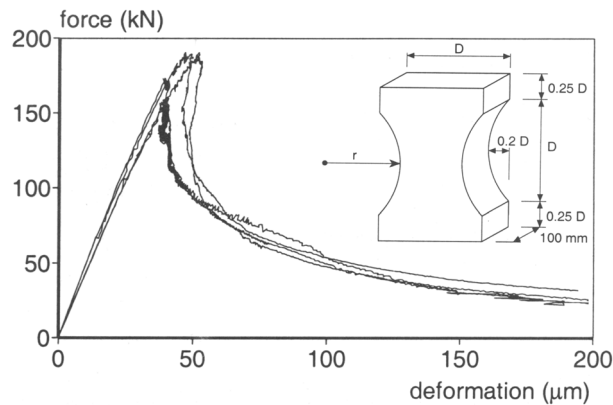


Fig. 6 Scheme of the dog-bone specimen and experimental load-displacement curves (van Vliet 2000)

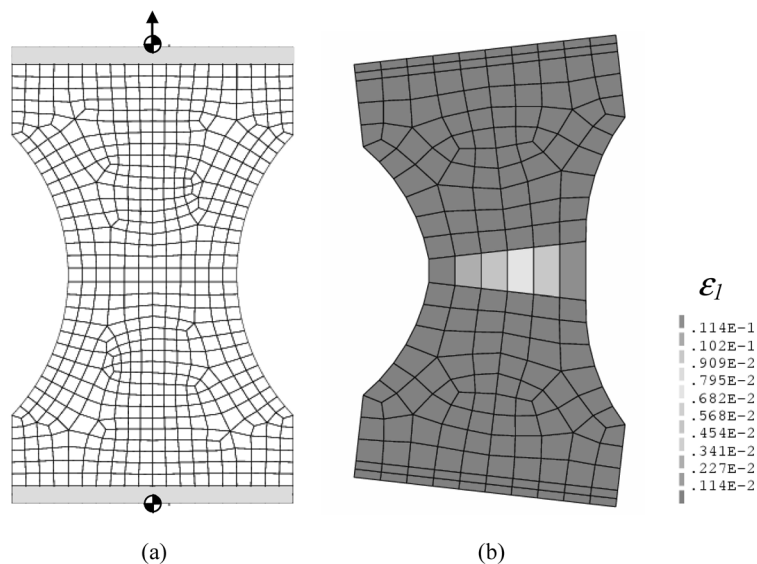


Fig. 7 Mesh of the dog bone specimen (a); deformed mesh and principal tensile strain contour referring to the last sequentially linear step (b)

3.1. *Smearred crack nonlinear analysis*

Prior to the sequentially linear analysis, a standard nonlinear analysis was performed. Linear iso-parametric plane stress elements were used to discretize both the plain concrete and the steel platens. The two element rows at top and bottom of Fig. 7(a) represent the steel platens. The boundary condition was carefully taken into account modeling the central hinges at top and bottom used to de-constrain the structure. The influence of the boundary condition on post peak behavior is crucial (van Vliet 2000), both from an experimental and numerical point of view. The experiment was performed under indirect crack displacement control and showed a pronounced snap-back, indicating stable crack propagation while both the load and the loading-point displacement decrease. The outcome of the numerical simulation depends on the control parameter. When the simulation is performed under load control, only the pre-peak branch of the load displacement curve can be traced. When the simulation is carried out under displacement control, the solution has to jump suddenly to a much lower equilibrium branch, which often fails. The third possibility is to adopt an indirect load control, e.g., an arc-length method based on a norm of all nodal displacements (Crisfield 1984) or a method based on a norm of a few selected nodal displacements, e.g., CMOD control over the active crack (de Borst 1987). Then, the entire load-displacement curve including the quasi-static snap-back can be obtained. Here, this approach was successful because only one clearly localized crack occurred. In general, however, the choice of load steps, arc-length options and indirect control parameters is quite cumbersome, and difficulties increase with increasing size of the structure (increasing brittleness) and with increasing number of propagating cracks (e.g. in reinforced situations).

Another problem with the nonlinear analysis is the bifurcation. In fact, as soon as the peak load is reached, due to the symmetry of the structure, two different equilibrium paths arise. The symmetric path is unstable, and is not encountered experimentally, while the non-symmetric stable path is characterized by crack propagation from one side only of the dog-bone specimen. Consequently, a negative pivot arises, in the LDU scheme, due to the bifurcation of equilibrium, and it is necessary to introduce a perturbation of symmetry (geometrical or material) in the model, in order to get a solution.

3.2. *Isotropic sequentially linear analysis*

The same mesh and the same mechanical parameters were adopted for the saw tooth analysis (Fig. 7a). The analysis was carried out with a ten-teeth approximation. The load displacement curve is depicted in Fig. 8, and shows a very good agreement with the smeared crack nonlinear analysis. It is worth noting that both curves compare well with experimental results. Each linear analysis gives a unique critical, scaled load-displacement set, i.e., a point in the load-displacement diagram. By connecting all these points, the sequentially linear response is obtained, again having a somewhat irregular but overall correct form. The advantage of the sequentially linear analysis is that the system is always positive definite, so that a solution is always found at each step. The sequence of linear solutions automatically provides the snap-back. When the solution is considered to be too coarse, it is possible to refine the mesh and/or to increase the number of teeth. For the present mesh, we have about five elements that are almost fully cracked, so that in total only about 5 times 10 (no. of teeth) linear analyses had to be executed. This is friendly to the user, as he is protected from selecting incremental-iterative schemes, step sizes and control techniques.

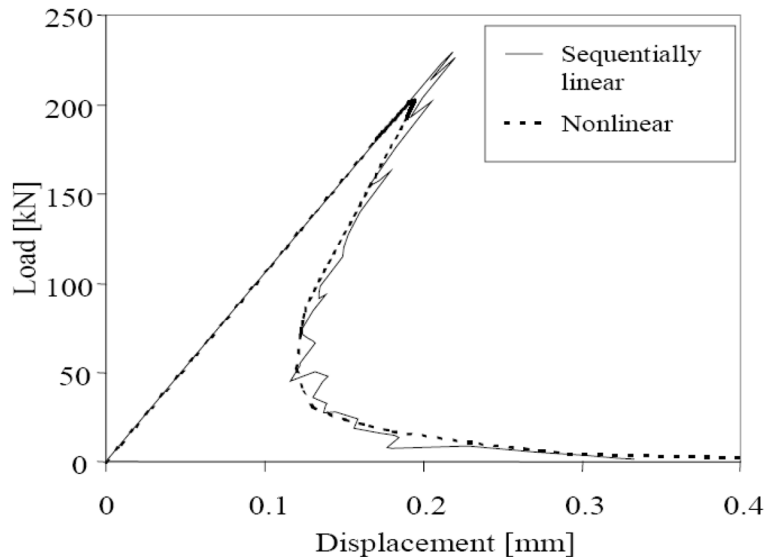


Fig. 8 Snap-back in the load displacement curve

Another advantage is that the scaling process mentioned in Section 2.1 involves that the numerical round-off implicitly breaks the symmetry of the model. There is no need to add imperfections to the model in order to follow the stable equilibrium path. At the same time, the indirect control of the structure is not required any more, since the effective control parameter is the propagating damage itself.

The sequentially linear simulation provides not only the correct load displacement curve, but also the correct non-symmetric damage localization in the central part of the sample, induced by the dog-bone shape of the specimen, as shown in Fig. 7(b).

4. Anisotropic sequentially linear: fixed cracking

In the previous section, and isotropic reduction of stiffness was assumed. Young's modulus was (saw-tooth wise) reduced in all directions. Although this isotropy assumption allows for the simulation of cracking of plane concrete in direct tension or bending (i.e. when the phenomenon is basically driven by a localized crack in a one-dimensional stress field), a substantial improvement is necessary when dealing with reinforced concrete. In fact the isotropic reduction of stiffness is a rather rough approximation, and does not represent the compressive struts that develop parallel to the cracks.

Therefore, in analogy to the pioneering approach of Rashid (1968), the initial isotropic stress-strain law can be replaced by an orthotropic law upon crack formation, with the axes of orthotropy being determined according to a condition of crack initiation. In the present work, the crack plane is kept fixed after crack initiation. Moreover, only one crack per element is considered.

Referring to the plane stress situation, and to a local coordinate system oriented parallel to the crack plane, the following constitutive relation is assumed (e.g. Rots, *et al.* 1985):

$$\begin{Bmatrix} \sigma_{nn} \\ \sigma_{tt} \\ \sigma_{nt} \end{Bmatrix} = \begin{bmatrix} \frac{E_i}{1-\nu^2 \frac{E_i}{E}} & \frac{\nu E_i}{1-\nu^2 \frac{E_i}{E}} & 0 \\ \frac{\nu E_i}{1-\nu^2 \frac{E_i}{E}} & \frac{E}{1-\nu^2 \frac{E_i}{E}} & 0 \\ 0 & 0 & \beta G \end{bmatrix} \begin{Bmatrix} \varepsilon_{nn} \\ \varepsilon_{tt} \\ \varepsilon_{nt} \end{Bmatrix} \quad (11)$$

where n is the normal to the crack, t the crack plane, E_i the reduced Young modulus according to the sequentially linear scheme, and β the so-called shear retention factor. This formulation is based on the work of Bažant and Oh (1983) extended with shear retention. Extension towards axi-symmetry, plane strain and 3D is straightforward. The equation can be rewritten in compact form as follows:

$$\boldsymbol{\sigma}_{nt} = \mathbf{D}_{nt} \boldsymbol{\varepsilon}_{nt} \quad (12)$$

In addition to Young's modulus, also the shear retention factor and Poisson's ratio are reduced with increasing crack opening. In the present implementation a stepwise reduction is assumed:

$$\begin{cases} \beta_i = \frac{N-i}{N} \\ \nu_i = \frac{N-i}{N} \end{cases}, \quad 0 \leq i \leq N \quad (13)$$

where i is the current tooth, and N the number of teeth adopted in the discretization. Given the following transformations for the strain and stress vectors:

$$\begin{cases} \boldsymbol{\varepsilon}_{nt} = \mathbf{T}_\varepsilon(\phi) \boldsymbol{\varepsilon}_{xy} \\ \boldsymbol{\sigma}_{nt} = \mathbf{T}_\sigma(\phi) \boldsymbol{\sigma}_{xy} \end{cases} \quad (14)$$

Eq. (12) can be easily transposed in terms of global stress and strain components by pre- and post-multiplication with the transformation matrices:

$$\boldsymbol{\sigma}_{xy} = \mathbf{T}_\sigma^{-1}(\phi) \mathbf{D}_{nt} \mathbf{T}_\varepsilon(\phi) \boldsymbol{\varepsilon}_{xy} \quad (15)$$

The above improved constitutive law was implemented in the general sequentially linear scheme. Below, three typical RC examples are shown, the third one being discussed in detail.

4.1. Reinforced tension-pull specimen

A long-embedment tension-pull specimen is considered (Gijsbers and Hehemann 1977). The length is 600 mm, the diameter of the rebar 8 mm and the diameter of the concrete 77 mm. The steel was modeled by truss elements, and the concrete by axi-symmetric elements. Perfect bond between steel and concrete was assumed. The strength of the concrete was assigned via a random generation of tensile strength (mean $f_t = 3.0$ MPa, standard deviation equal to 0.5 MPa). A long-embedment RC specimen is a challenging test case due to the existence of an undisturbed zone of

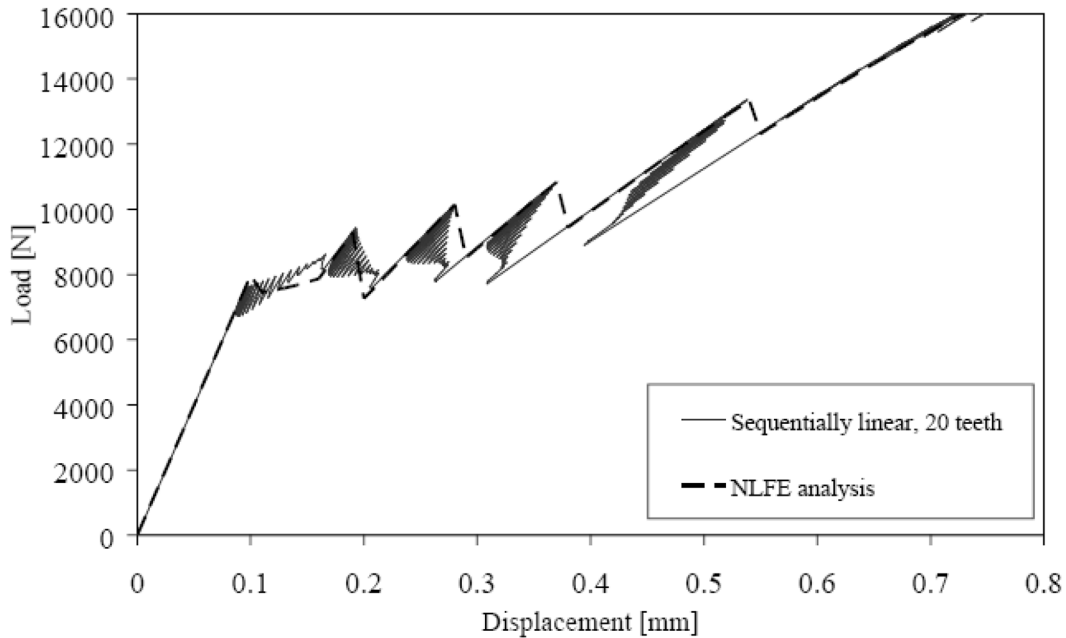


Fig. 9 Load-displacement curves: experimental (Gijsbers and Hehemann 1977), nonlinear (Rots 1985) and sequentially linear analysis

homogeneous tensile stress in the central part of the specimen. This involves the initiation of multiple cracks that compete to survive. In such cases, incremental-iterative nonlinear procedures may fail due to the existence of alternative equilibrium states (Crisfield 1984). The specimen was analysed before by Rots (1988) under indirect displacement control, leading to four snap-backs associated with four primary cracks. The problems with alternative equilibrium states were avoided by using very small steps, strength perturbations and delicate choice of steering parameters.

Fig. 9 compares results from nonlinear smeared analysis with the load-displacement curve for the anisotropic sequentially linear model. Here, the nonlinear analysis was performed under displacement control, showing four un-converged jump-overs associated with the four primary cracks. Obviously, for this particular example stable situations with new ascending paths were recovered beyond the un-converged drops, which cannot be guaranteed in general circumstances. In fact the nonlinear response is a 'saw-tooth' response at macro-level. The sequentially linear analysis, based on saw-tooth input at micro-level, is in good agreement with the nonlinear results, but in addition appears to be able to describe the snap-through and snap-back behavior for the four primary crack events. The brittle snap behavior is obtained automatically, as a sequence of linear states. In Fig. 10, the comparison is made in terms of crack localization and resulting deformed meshes. Four primary cracks emerge. In particular, Fig. 10(c) shows how compressive struts arise in the anisotropic saw-tooth analysis. These cone-shaped struts in the axi-symmetric setting are balanced against tangential tensile rings. With the former isotropic version of the model, the struts (compressive cones) could not develop and an incorrect crack evolution was obtained.

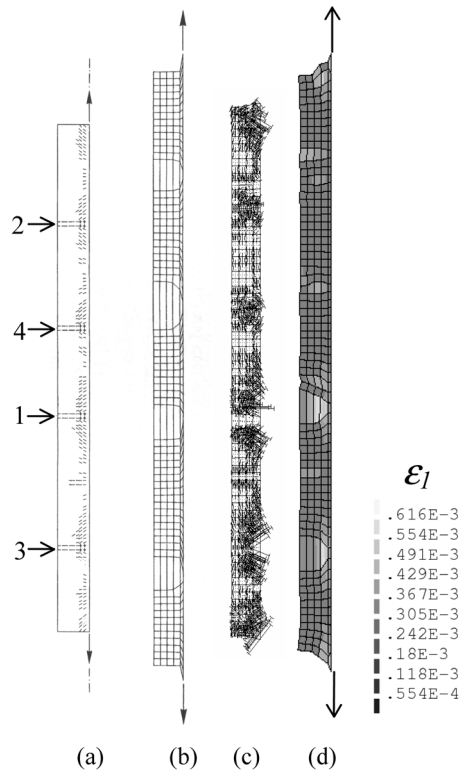


Fig. 10 Long-embedment tension-pull specimen. Nonlinear cracking (a), nonlinear deformed mesh (b). Sequentially linear compressive struts (c) and deformation (d)

4.2. Reinforced concrete beam

The RC tension-pull specimen can be seen as a part of an RC structure. Then the saw-tooth macro output for the individual RC tensile zone becomes integral part of the response of a full structure having multiple of these zones. In this example we investigate the performance of the anisotropic saw-tooth model with respect to a reinforced beam which fails in bending and which was tested by Walraven (1978). The geometry and finite element idealization for the beam is shown in Fig. 11. Eight-noded plane-stress elements were used to represent the concrete and three-noded truss element for the reinforcement. Perfect bond was assumed between the concrete and

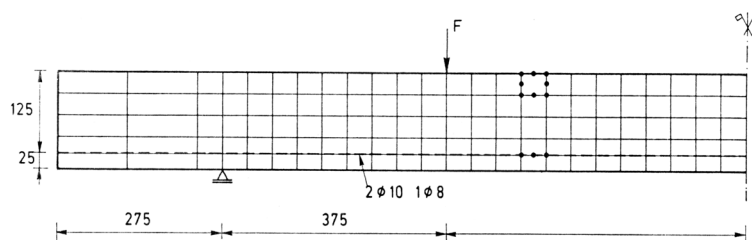


Fig. 11 Finite element idealization of the RC beam

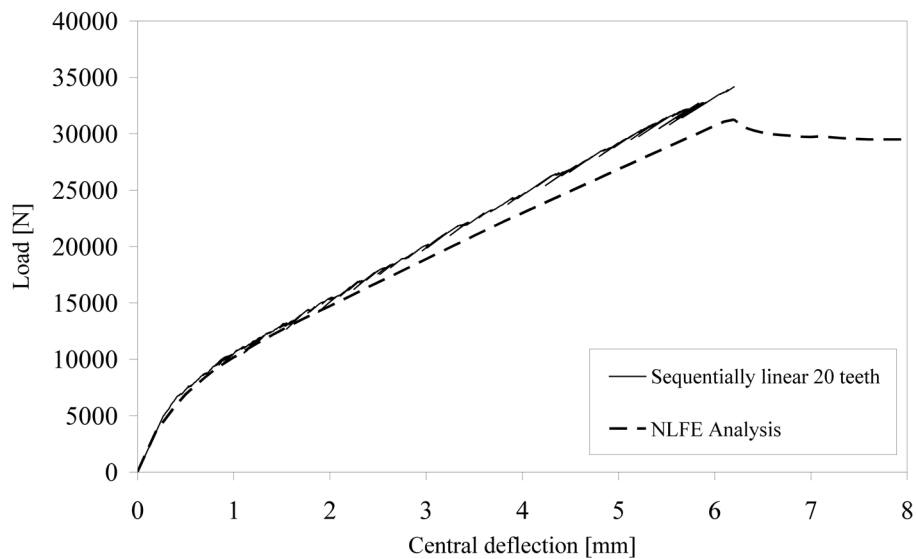


Fig. 12 Load-displacement curves: nonlinear (Rots 1985) and sequentially linear analysis

reinforcement. Both a nonlinear smeared crack and an anisotropic sequentially linear analysis were performed. The results in Fig. 12 show agreement between the sequentially linear and nonlinear or experimental data. Near the end of the sequentially linear curve, the intensity of the ripples and valleys becomes more pronounced, indicating a transition from stable bending cracks in the central zone to more brittle diagonal shear cracks between support and loading point.

In this sequentially linear analysis the yielding of the reinforcement has not yet been taken into account, whereas in the nonlinear analysis it was, giving the limit plateau. The emphasis here is on demonstrating that the sequentially linear method is numerically stable and able to pass the individual localizations of both bending and shear cracks in the reinforced structure. However, an extension of the model to include steel yielding is possible by taking a discretized saw-tooth approximation of the elasto-plastic steel stress-strain curve in addition to the saw-tooth approximation of the concrete tensile stress-strain softening curve (Rots, *et al.* 2006). Similarly, non-linearity of concrete in compression can be added, by taking a saw-tooth discretization of the parabolic concrete compressive stress-strain curve.

For both this RC beam and the tension-pull specimen, the predicted envelope curves in Figs. 9 and 12 appear to be locally weaker than the experimental curves. This difference may be due to incorrect choices of the precise material parameters. A sensitivity study and quantitative matching of the experimental results has not yet been carried out, as it was not the prime interest in this stage.

4.3. One-way slab of Jain and Kennedy

A one-way slab, effectively a beam, tested by Jain and Kennedy (1974), has been analyzed. This example will be described in detail. The simply supported slab was 760 mm long, 460 mm wide and 38 mm thick. A uniaxial moment was generated by means of two uniformly distributed line loads across the slab width, symmetrically placed at 150 mm from each support. The slab was

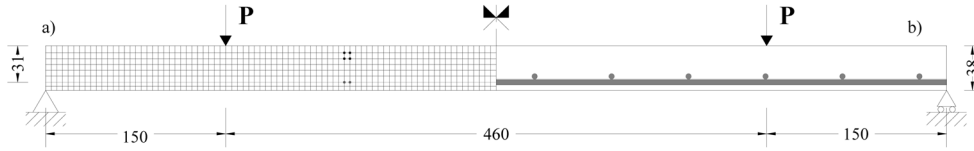


Fig. 13 Finite element idealization (a) and Experimental set up (b) [mm]

isotropically reinforced with the first layer of steel placed at 4.8 mm clear cover, while the second layer was orthogonal to the first and placed directly over the first layer. Plain mild steel BB rods with a diameter equal to 4.8 mm and a spacing equal to 65 mm were used, providing a reinforcement ratio of 0.00716. Fig. 13 shows the experimental set up and the finite element idealization. A plane-stress assumption was made, but extension to plate/shell elements is straightforward. Four-node elements were used for the concrete and two-node trusses for the reinforcement with perfect bond. Both nonlinear smeared crack and an-isotropic sequentially linear analyses were performed.

In the nonlinear analyses, two different fixed smeared crack models were employed, based on the concept of total-strain and decomposed strain respectively (e.g. Rots, *et al.* 1985, Feenstra, *et al.* 1998). The expected slab failure mode is steel yielding. Therefore, the compression non-linearity of the concrete has been ignored. Only tensile cracking has been included and elastic-plastic behavior of the reinforcement. The parameters for this slab have been taken from Gilbert and Warner (Gilbert and Warner 1978), tensile strength 2 MPa and Young's modulus 29000 MPa for the concrete and yield stress 220 MPa and Young's modulus 200000 MPa for the steel. A constant shear retention factor equal to 0.2 describes the shear behavior of fixed cracks. The mechanisms that transmit forces across cracks in RC have been modeled by an average tension-stiffening stress-strain relationship for concrete in tension. The usual assumption is that the stress carrying capacity of the reinforced concrete gradually decreases and is exhausted once the reinforcement starts yielding. This implies that the ultimate strain ϵ_u of the tension-stiffening curve equals the yield strain ϵ_{ys} of the steel rebars. Here, the actual nonlinear curve has been approximated by a linear curve with an ultimate strain of 70% of the nonlinear curve, Fig. 14, giving $\epsilon_u = 0.7 \times (220/200000) = 0.7 \times 0.0011 = 0.00077$. When this ultimate strain would be interpreted in the spirit of tension-softening

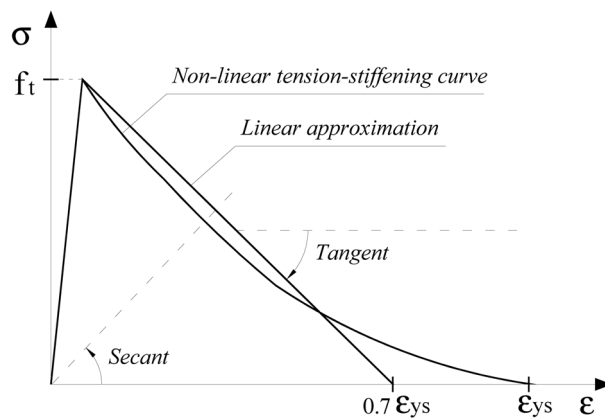


Fig. 14 Tension stiffening formulation: schematic plot and linear approximation

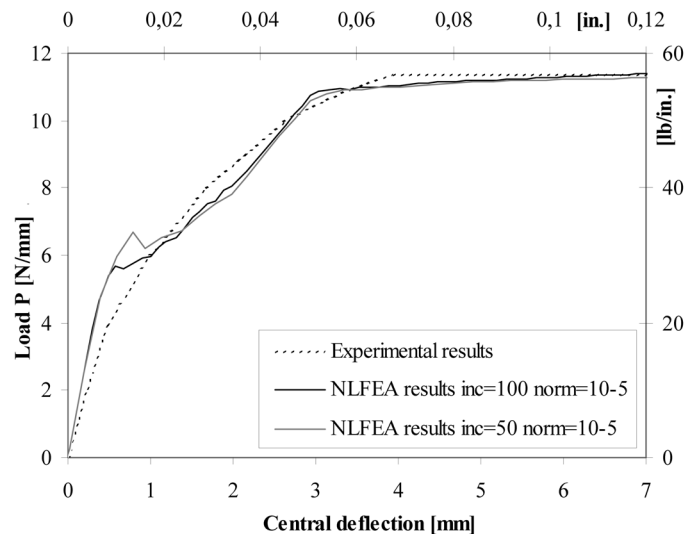


Fig. 15 Load versus central deflection - Nonlinear results, two different step sizes, total-strain crack model

for localized cracks, it would relate to a fracture energy G_f of 0.0037 N/mm over the crack band width (element length in this case) of 4.75 mm. The nonlinear analyses were carried out under displacement control using regular Newton-Raphson, with an energy norm convergence tolerance of 10^{-5} , a maximum number of 100 iterations, and for two different increments sizes (100 increments of 0.06 mm and 50 increments of 0.12 mm). Load-displacement responses for the nonlinear analyses are shown in Fig. 15.

First, the tangent stiffness for the Newton-Raphson procedure at structural level was based on the pure, negative tangent stiffness of the stress-strain curves at local level. With this approach, negative pivots occurred immediately upon initial cracking and convergence could not be achieved, or more precise, divergence occurred. Reduction of displacement increments or use of arc-length schemes could not eliminate these problems. Subsequently, the tangent stiffness at structural level was based upon the positive secant stiffness of the stress-strain curves at local level, with results shown in Fig. 15. With this approach, convergence on the norm could be achieved in all steps. However, this 'convergence' was slow and it certainly was not a quadratic convergence. Especially, the range between 0.5 and 2 mm deflection appeared to be critical. To study this, some options were varied. First, the energy norm was tightened from 10^{-5} to 10^{-7} . Then, slight differences in the load-displacement solution occurred and convergence could not be achieved in 5 steps. Second, the displacement increments were doubled and halved. Again, the results turned out to be different, i.e. non-unique. For 50 instead of 100 increments, the norm of 10^{-7} resulted in 4 un-converged steps. Thirdly, a decomposed-strain based smeared crack model was used instead of the total-strain based model. Then, more un-converged states were found, namely in 7 steps for the case of 50 increments and in 11 steps for the case of 100 increments. This poorer convergence behavior maybe due to the fact that the decomposed model requires internal iterations whereas the total-strain model is in a way explicit and therefore more robust.

The conclusion is that the nonlinear results are clearly non-unique and in-objective with respect to step sizes and convergence criteria adopted. The reason lies in the presence of alternative equilibrium states, associated with multiple cracks that compete to survive. Many cracks are initiated, but only a

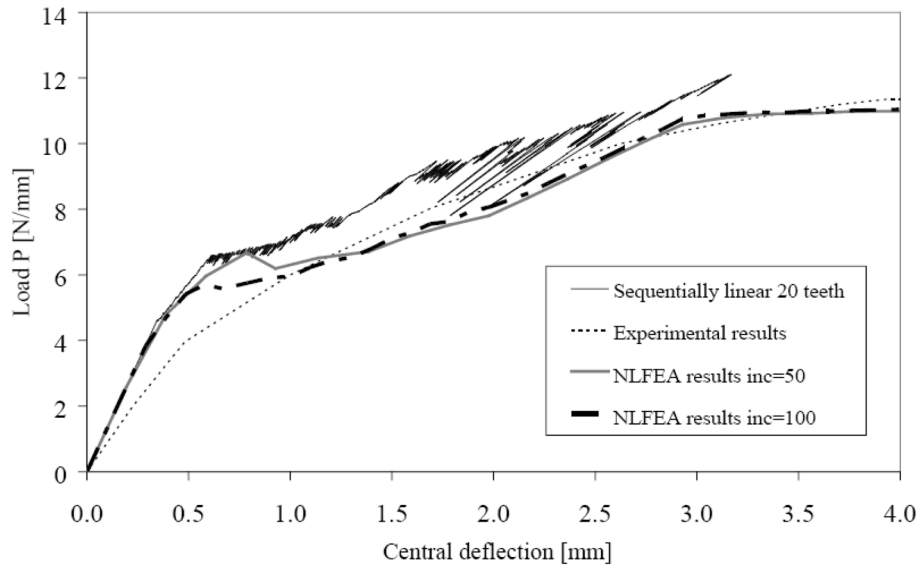


Fig. 16 Sequentially linear analysis (20 teeth)

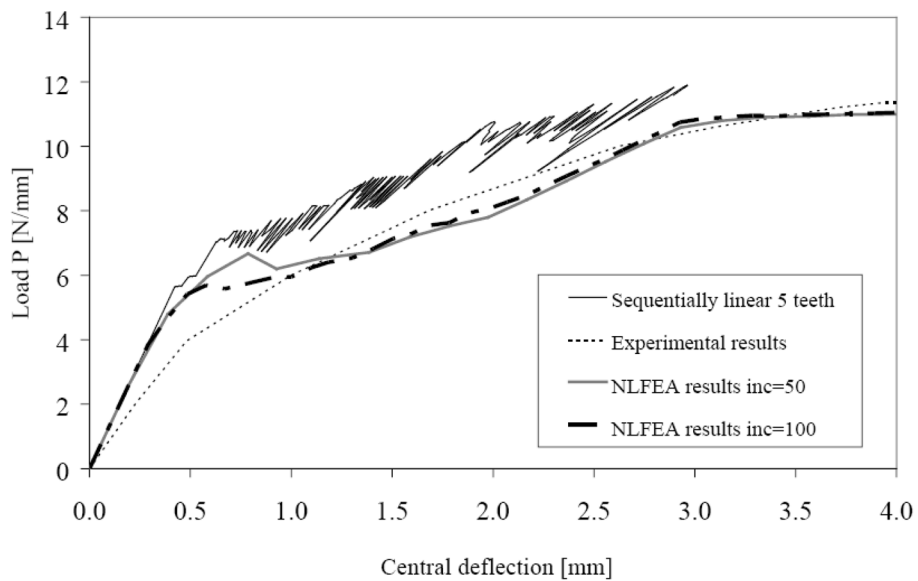


Fig. 17 Sequentially linear analysis (5 teeth)

few of them can proceed whereas others unload (e.g. Crisfield 1982). This selection and survival process gives bifurcations and divergence when using tangent stiffness and ‘insufficient convergence’ when using secant stiffness.

As an alternative, the same beam with the same parameters was analyzed in the sequentially linear fashion. The fixed anisotropic formulation described in chapter 4 was adopted, i.e., the saw-tooth reduction of strength and stiffness was applied in the direction normal to the initial crack direction (Rots and Invernizzi 2004a). This makes the result comparable to the nonlinear fixed

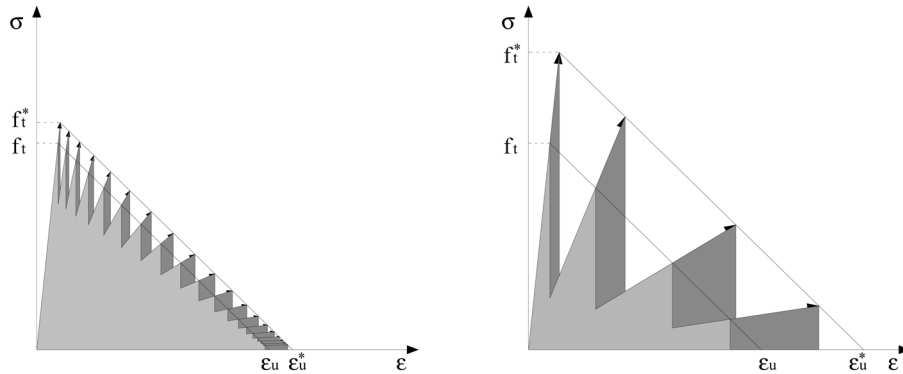


Fig. 18 Saw-tooth approximation of linear softening/stiffening curve. Left: twenty teeth. Right: five teeth

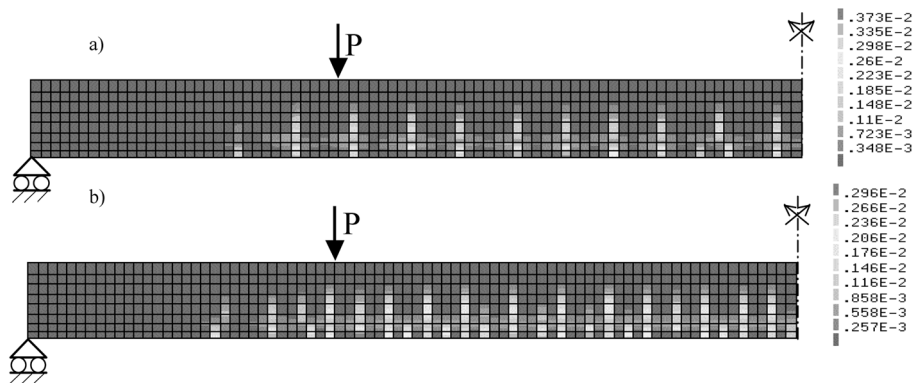


Fig. 19 Principal tensile strains at central deflection 2.5 mm. (a) sequentially linear 20 teeth, (b) nonlinear

smear crack results. The previous version of the saw-tooth model assumed isotropic degradation, but this would result in a too soft behavior for RC beams and slabs. In order to achieve mesh-objectivity, the envelope curve was again uplifted such that the area under the uplifted saw-tooth diagram is the same as the area under the original envelope diagram, Fig. 18. This keeps the energy invariant and the result mesh-objective as well as objective with respect to the number of saw-teeth adopted (Rots and Invernizzi 2004b). The result for the slab is shown in Fig. 16 (twenty teeth) and Fig. 17 (five teeth). Each linear analysis gives a scaled critical load-displacement point. The load-displacement curve is constructed by connecting all these points from all linear analyses. The process of linear analysis, critical element selection, strength/stiffness reduction for that element according to the saw-tooth curve, subsequent linear analysis, etc. was automated. The results prove that the method is able to represent the load-displacement response for RC slabs sufficiently accurate compared to the nonlinear analyses. The ripples (Crisfield 1982) or local snap-backs typical for RC structures appear automatically. There are no problems with alternative equilibrium states or bifurcations as the scaling procedure always picks the ‘lowest’ solution. The approach always ‘converges’. It is just a sequence of positive-definite linear-elastic analyses, which is simple, effective and robust.

The results also show sufficient objectivity with respect to the number of teeth adopted. The twenty-teeth solution gives a somewhat smoother response curve than the five-teeth solution.

Considering that the five-teeth approximation is quite rough (Fig. 18), the result is still remarkably good. Fig. 19 gives principal strain patterns, reflecting the cracks. The sequentially linear solution provides a better localization of the cracks, while the nonlinear analysis shows some checkerboard pattern around the rebar, indicating bifurcation and hesitation of cracks to localize. Other examples and backgrounds of the model can be found in Rots (2001), Rots and Invernizzi (2004a, b).

All numerical results in this section are initially stiffer than the experimental result. This aspect has not yet been investigated, but is likely to be due to an overestimation of the Young's modulus in the analyses, or by possible initial displacements in the experimental set-up.

5. Conclusions

A sequentially linear continuum model is presented as an alternative to nonlinear softening continuum models. The softening diagram of negative slope is replaced by a saw-tooth diagram of positive slopes. The incremental-iterative Newton method is replaced by a series of linear analyses using a special scaling technique with subsequent stiffness/strength reduction per critical element. It has been shown that this event-by-event strategy is robust and reliable. The method fits the thinking of RC practicing engineers, who often account for cracking by pragmatically reducing the bending stiffness in certain areas, and then repeat their linear analyses. The saw-tooth model does a similar thing, but then at local finite element level.

First, the example of a large-scale dog-bone specimen in direct tension has been analyzed using an isotropic version of the saw-tooth model. The model is capable of automatically providing the snap-back response and it circumvents difficulties due to the symmetric/non-symmetric bifurcation. Next, the saw-tooth model has been extended to include anisotropy for fixed crack directions to accommodate both tensile cracking and compression strut action for reinforced concrete. Three different reinforced concrete structures have been analyzed, a tension-pull specimen, a slender beam and a slab. The latter example has been discussed in detail. In all cases, the model naturally provides the local peaks and snap-backs associated with the subsequent development of primary cracks starting from the rebar. The secant saw-tooth stiffness is always positive and the analysis always 'converges'. Bifurcations are prevented due to the scaling technique.

References

- Bazant, Z.P., and Cedolin, L. (1979), "Blunt crack band propagation in finite element analysis", *J. Eng. Mech. Div., ASCE*, **105**(2), 297-315.
- Bazant, Z.P., and Oh, B.H. (1983), "Crack band theory for fracture of concrete", *Mater. Struct.*, **16**(93), 155-177.
- Beranek, W.J., and Hobbelman, G.J. (1995), "2D and 3D-Modelling of concrete as an assemblage of spheres: reevaluation of the failure criterion", *Fracture Mechanics of Concrete Structures. Proc. FRAMCOS-2*, Wittmann F.H. (ed.), Freiburg: Aedificatio, 965-978.
- Carpinteri, A., (1986), *Mechanical Damage and Crack Growth in Concrete: Plastic Collapse to Brittle Fracture*. Martinus Nijhoff Publishers, Dordrecht.
- Carpinteri, A., Monetto, I. (1999), "Snap-back analysis of fracture evolution in multi-cracked solids using boundary element method", *Int. J. Fracture*, **98**, 225-241.
- Crisfield, M.A. (1982), "Accelerated solution techniques and concrete cracking", *Comput. Methods Appl. Mech. Eng.*, **33**, 585-607.

- Crisfield, M.A. (1984), "Difficulties with current numerical models for reinforced-concrete and some tentative solutions", *Proc. Int. Conf. Computer Aided Analysis and Design of Concrete Structures*, **I**, 331-358 F. Damjanic, N. Bicanic *et al.* (eds).
- De Borst, R. (1987), "Computation of post-bifurcation and post-failure behaviour of strain-softening solids", *Comp. Struct.*, **25**(2), 211-224.
- Feenstra, P.H., Rots, J.G., Arnesen, A., Teigen, J.G., Hoiseth, K.V. (1998) "A 3D constitutive model for concrete based on a co-rotational crack concept", *Computational Modelling of Concrete Structures, Proc. EURO-C 1998*. De Borst *et al.* (eds), Balkema: Rotterdam, 13-22.
- Gijsbers, F.B.J., and Hehemann, A.A. (1977), "Some tensile tests on reinforced concrete", *Report BI-77-61*, TNO Inst. For Building Mat. And Struct., Delft.
- Gilbert, R.I., and Warner, R. F. (1978), "Tension stiffening in reinforced concrete slabs", *J. Struct. Div., ASCE*, **104**(12), 1885-1900.
- Jain, S.C., and Kennedy, J.B. (1974), "Yield criterion for reinforced concrete slabs", *J. Struct. Div., ASCE*, **100**(3), 631-644.
- Rashid, Y.R. (1968), "Analysis of prestressed concrete pressure vessels", *Nuclear Eng. Design*, **7**(4), 334-344.
- Rots, J.G. (1988), "Computational modeling of concrete fracture", Ph.D. Thesis, Delft University of Technology, Delft, The Netherlands.
- Rots, J.G. (2001), "Sequentially linear continuum model for concrete fracture", *Fracture Mechanics of Concrete Structures, Proc. FRAMCOS-4*, de Borst R, Mazars J, Pijaudier-Cabot G, van Mier JGM, Balkema AA (eds). Lisse: The Netherlands, 831-839.
- Rots, J.G., Belletti, B., Invernizzi, S. (2006) "Simplified saw-tooth softening model for reinforced concrete structures", *Proceedings of the 2nd International FIB Congress*, 5-8 June, Napoli, Italy.
- Rots, J.G., and Invernizzi, S. (2003), "Regularized saw-tooth softening", *Computational Modelling of Concrete Structures*, Lisse: Balkema, 599-617 Bićanic N., de Borst R., Mang H., Meschke G. (eds).
- Rots, J.G. and Invernizzi, S. (2004a), "Saw-tooth softening/stiffening model", *Fracture Mechanics of Concrete Structures*, Li VC, Leung C, Willam K, Billington S (eds). *Proc. FraMCoS-5, 1a FraMCoS-5: USA*, 375-382.
- Rots, J.G., and Invernizzi, S. (2004b), "Regularized sequentially linear saw-tooth softening model", *Int. J. Numer. Anal. Methods Geomech*, **28**, 821-856.
- Rots, J.G., Nauta, P., Kusters, G.M.A., Blaauwendraad, J. (1985), "Smearred crack approach and fracture localization in concrete", *HERON*, **30**(1), 1-48.
- Schlangen, E., and van Mier, J.G.M. (1992), "Experimental and numerical analysis of micro-mechanisms of fracture of cement-based composites", *Cem. Conc. Compo.*, **14**, 105-118.
- Van Vliet M.R.A. (2000), "Size effect in tensile fracture of concrete and rock", PhD thesis TU Delft, Faculty of Civil Engineering, Delft University Press, Delft, The Netherlands.
- Walraven, J.C. (1978), "The influence of depth on the shear strength of lightweight concrete beams without shear reinforcement", Report 5-78-4 Stevin Laboratory, Delft University of Technology, Delft.